Article ID: 1003－6326(2005)01－0087－06

In-plane anisotropy of 1545 aluminum alloy sheet①

PENG Yong-yi(彭勇宜)[1,2], YIN Zhi-min(尹志民)[2],
YANG Jin(杨 进)[2], DU Yu-xuan(杜予晅)[2]
(1. School of Physics Science and Technology,
Central South University, Changsha 410083, China;
2. School of Materials Science and Engineering,
Central South University, Changsha 410083, China)

Abstract: The microstructures and the tensile mechanical properties in the rolling plane of 1545 aluminum alloy sheet at different orientations with respect to the rolling direction were studied by means of tensile test, X-ray diffractometer(XRD), optical microscope and transmission electron microscope. The in-plane anisotropy of tensile mechanical properties was calculated and the inverse pole figures of the rolling plane, transversal section and longitudinal section were obtained by Harris method. The results show that the 1545 Al alloy sheet has remarkable in-plane anisotropy of mechanical properties and the main texture component is {110}〈112〉 texture. On the basis of the model that regards the sheet containing only {110}〈112〉 texture as a monocrystal, the relationship of in-plane anisotropy and the anisotropy of crystallography was analyzed. The study shows that it is the combined effects of the anisotropy of crystallography and microstructures that cause the in-plane anisotropy of mechanical properties, but the main cause is the crystallographic texture.

Key words: 1545 alloy aluminum sheet; in-plane anisotropy; inverse pole figure; crystallographic texture
CLC number: TG 146.2 **Document code:** A

1 INTRODUCTION

The in-plane anisotropy of mechanical properties brings the limitation to the use of alloy sheet. At the same time, during the material processing, the difficulties of contour machining will also be increased. For this reason, when designing high-performance aluminum alloy sheets, the in-plane anisotropy is an important performance parameter that must be considered. Studies have shown that minor Sc and Zr in the Al-Mg-Mn alloy can refine grains of cast ingot, inhibit recrystallization in the course of hot deformation and annealing after cool-working, and enhance the strength and plasticity of the alloy sheets[1-5]. The aluminum alloy containing minor Sc and Zr has excellent corrosion resistance, weldability, fatigue fracture resistance and high-temperature stability[6-9], so it is a kind of neotype and light-mass structural material used in aerospace and aviation application. However, there is little investigation about in-plane anisotropy of aluminum alloy sheets which contain minor Sc and Zr up to now. This article discloses the apparent laws of in-plane anisotropy of mechanical properties in 1545 aluminum alloy sheet, analyzes and discusses the causes of in-plane anisotropy from two aspects: the anisotropy of microscopic structure, and the crystallographic texture.

2 EXPERIMENTAL

2.1 Material

The nominal compositions of experimental aluminum alloy sheet are listed in Table 1. The alloy ingot was produced by semi-continuous casting technique. The 3.4 mm-thick sheet was annealed for stabilization at 340 ℃ for 1 h in the end.

Table 1 Nominal compositions of experimental alloy sheet (mass fraction, %)

Element	Mg	Mn	Sc	Zr	Al
Content	5.2	0.3	0.25	0.12	Balance

2.2 Experimental methods

2.2.1 Testing of tensile mechanical properties

Tensile test specimens were machined from the annealed aluminum alloy sheet at 0°, 30°, 45°, 60°, 90° with respect to the rolling direction in the rolling plane. Fig. 1 shows the tensile specimens of different orientation in the rolling plane. The size of tensile specimens and the tensile test were accorded to GB6397—86 and GB228—87, respectively. Specimens were tested on CSS-44100 tensile testing machine and the ratio was 2 mm/min.

2.2.2 Calculation of IPA

① **Foundation item:** Project (G19999064911) supported by the National Key Fundamental Research Development Program of China
Received date: 2004－07－30; **Accepted date:** 2004－12－01
Correspondence: PENG Yong-yi, PhD candidate; Tel: +86-731-8836276; E-mail: pengyongyi@126.com

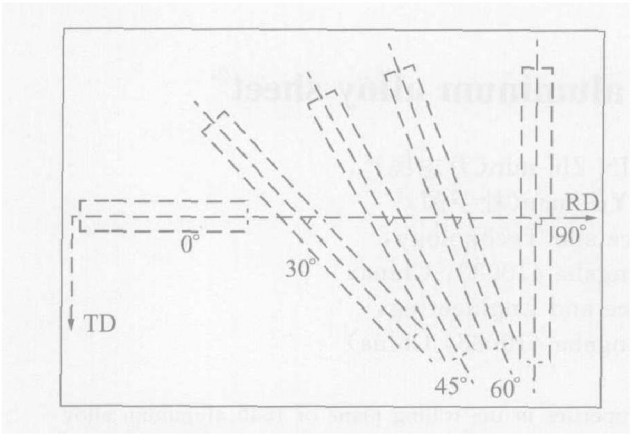

Fig. 1 Tensile specimens of different orientation in rolling plane of sheet
(RD—Rolling direction; TD—Transverse direction)

The method of calculation introduced by Refs. [10-13] was employed, and the IPA (in-plane anisotropy, A_{IP}/%) of each mechanical property was calculated using the equation:

$$A_{IP} = \frac{4X_{max} - X_{mid1} - X_{mid2} - X_{mid3} - X_{min}}{4X_{max}} \quad (1)$$

where X_{max} and X_{min} are the maximum and minimum of each mechanical property, respectively. X_{mid1}, X_{mid2} and X_{mid3} are between X_{max} and X_{min}.

2.2.3 Measurement of inverse pole figures

The experimental sheet was thin, and in order to obtain accurate X-ray diffraction experimental data of the transverse section and the longitudinal section, a combined specimen that was overlapped by four small test samples was prepared for the measurement of XRD. The X-ray diffraction patterns of the rolling plane, transverse section and longitudinal section were obtained on D/max 2000 rotaflex X-ray diffractometer (18 kW) and Cu K_α radiation was adopted. In the data processing, Harris method revised by Horta was employed, namely, P_{HKL} were calculated using equation(2)[14]. Then, the inverse pole figures of rolling plane, transverse section and longitudinal section were drawn.

$$P_{HKL} = \frac{I_{HKL}}{I_{S,\,HKL}} \Big/ \frac{\sum_1^n \left[N_{HKL} \frac{I_{HKL}}{I_{S,\,HKL}} \right]}{\sum_1^n N_{HKL}} \quad (2)$$

2.2.4 Observations of microstructure

The metallographic specimens taken from the rolling plane, transverse section and longitudinal section, treated by electrolytic polishing and anodizing membrane with solution which was composed of 30 mL HF, 11 g H_3BO_3 and 970 mL water, later were examined for observing grain structure on Ployvar-Met under polarized light. The voltage of electrolytic polishing and anodizing membrane was 20 V and 15 V, respectively. Thin foils for TEM observation were prepared by twin-jet polishing with an electrolyte solution consisting of 4% $HClO_4$ and 96% C_2H_5OH below −20 ℃, and the voltage and current for twin-jet polishing were 45 V and 30 mA, respectively. The foils were observed on Hitachi-800 electron microscope.

3 EXPERIMENTAL RESULTS

3.1 Tensile mechanical properties of sheet at different orientations

Tensile mechanical properties of sheet at different orientations are shown in Table 2 and Fig. 2.

Table 2 Tensile mechanical properties of sheet at different orientations and their in-plane anisotropy

Orientation	σ_b/MPa	$\sigma_{0.2}$/MPa	δ_5/%
0°	420	305	13.2
30°	410	301	17.3
45°	385	263	25.3
60°	381	272	23.2
90°	423	322	20.7
A_{IP}/%	5.7	11.4	26.5

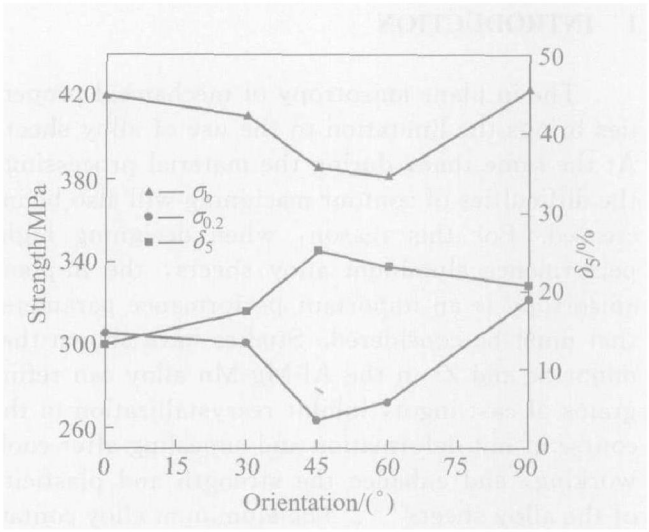

Fig. 2 Orientation dependence of tensile mechanical properties

Table 2 and Fig. 2 show the variations in tensile mechanical properties as a function of specimen orientation with respect to the rolling direction. It can be seen that, the yield strength varies with the specimen orientation, reaching the minimum at 45° to the rolling direction. The elongation also varies with the specimen orientation, reaching the maximum of 25.3%. The in-plane anisotropy of $\sigma_{0.2}$ and δ_5 is higher than that of σ_b.

3.2 Inverse pole figures of alloy sheet

Fig. 3 shows the inverse pole figures determined by Harris method.

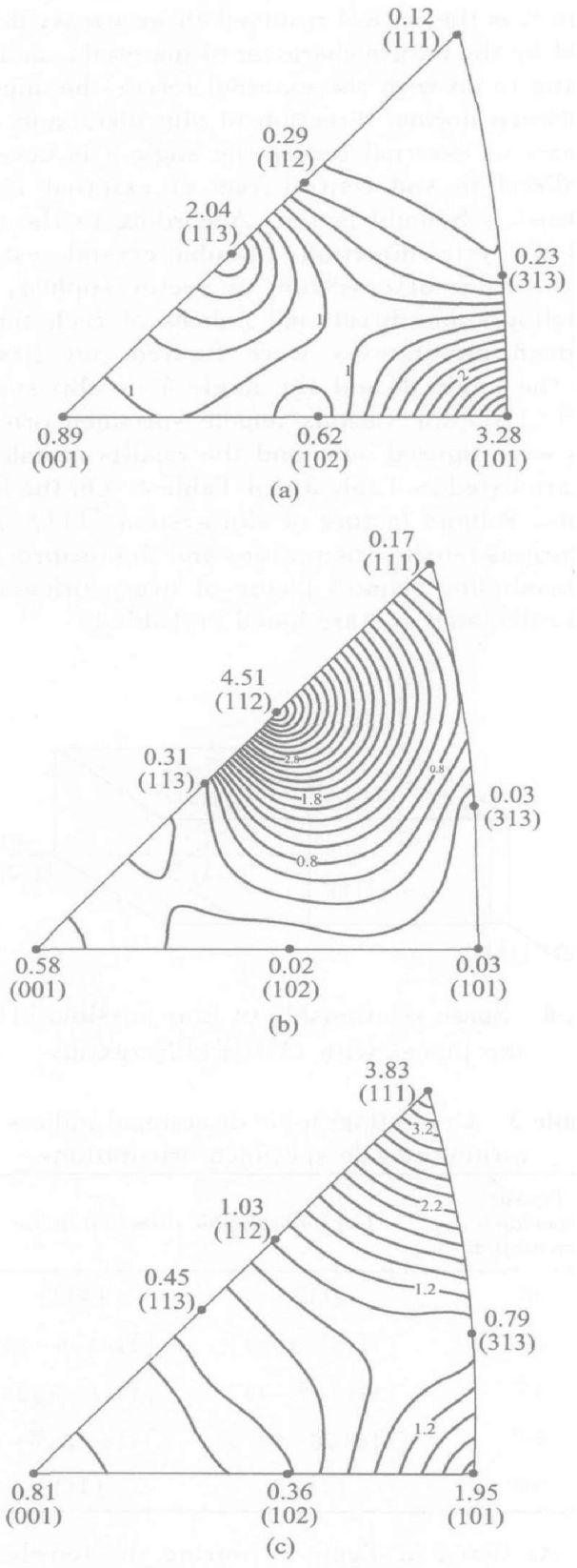

Fig. 3 Inverse pole figures of different planes of alloy sheet
(a) —Rolling plane; (b) —Transverse section; (c) —Longitudinal section

Fig. 3 indicates that the majority of {101} crystal plane and the minority of {113} crystal plane are parallel to the rolling plane, the majority of ⟨112⟩ crystal direction are parallel to the rolling direction, and the majority of ⟨111⟩ and ⟨101⟩ crystal direction are parallel to the transverse direction. The values of axis density are compared, and it can be found that the major component of texture in the 1545 alloy sheet is the {110} ⟨112⟩ texture.

3.3 Metallographic microstructures of alloy sheet

The metallographic microstructures of alloy sheet are shown in Fig. 4. The alloy sheet remains the deformed fibrous microstructures after annealing, and the metallographic microstructures look like pancake.

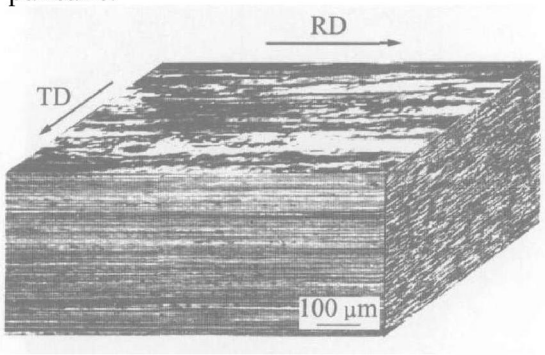

Fig. 4 Metallographic microstructures of alloy sheet
(RD —Rooling direction; TD —Transverse direction)

3.4 TEM microstructures of alloy sheet

The TEM micrographs of 1545 alloy sheet are shown in Fig. 5. A number of subgrains exist in the annealed sheet, which shows that recrystallization does not happen in the alloy (Fig. 5(a)). Under high magnification, it can be seen that nanometer Al_3(Sc, Zr) particles precipitate. These particles strongly pin the dislocations and subgrain boundaries, and inhibit the recrystallization (Fig. 5 (b)).

4 ANALYSIS AND DISCUSSION

The in-plane anisotropy of σ_b, $\sigma_{0.2}$ and δ_5 is high in the 1545 aluminum alloy sheet containing Sc and Zr, namely, this alloy sheet has remarkable in-plane anisotropy. It is assumed that it is induced by the complex interaction between microstructures and crystallographic texture. First, the microstructures of 1545 alloy sheet are elongated along the rolling direction (Fig. 4). The anisotropy of this kind of grain morphology should induce the anisotropy of mechanical properties. Because the grain boundary density along the transverse direction is greater than that along the rolling direction, the average value of grain diameter along the transverse direction is smaller than that along the rolling direction. It also indicates that different tensile orientations have different grain boundary densities which are passed through by the axis of external force in the tensile test. According to Hall-Petch

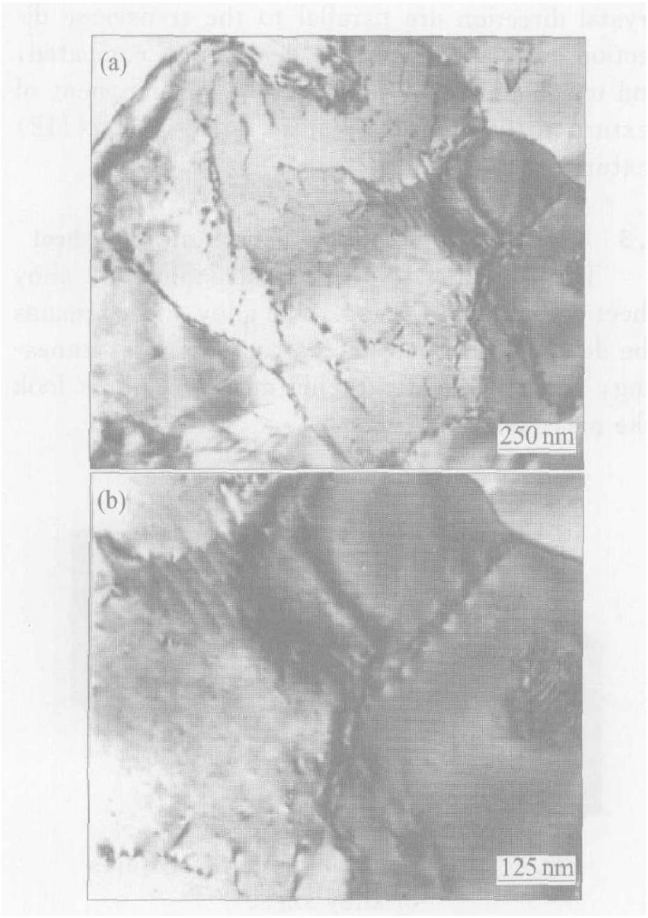

Fig. 5 TEM images of 1545 Al alloy sheet

formula $\sigma_s = \sigma_0 + Kd^{-1/2}$, the transverse (90°) strength could be higher than the longitudinal (0°) strength. Second, precipitation strengthening phases $Al_3(Sc, Zr)$ particles in this alloy sheet prevent effectively the migration of grain boundaries during hot rolling, hence, recrystallization is inhibited. For this reason, strong crystallographic texture comes into being. The anisotropy of crystallography can induce the anisotropy of mechanical properties.

The analysis of the inverse pole figures indicates that the major component of texture in the alloy sheet is the {110}〈112〉 texture. In order to simplify the problem, it is assumed that the sheet has a perfect (110)[$1\bar{1}2$] texture, and the alloy sheet is looked on as a monocrystal. Fig. 6 shows the relationship of the macro-coordinate system (the rolling direction, the transverse direction and the normal direction) with the coordinate system of crystal orientation ((110)[$1\bar{1}2$]). The crystal structure of aluminum alloy is face-centered cube, and its major slip system is {111}〈110〉. The space relationship of the four possible {111} slip planes with (110)[$1\bar{1}2$] texture is shown in Fig. 6 also. Two of the four possible {111} slip planes are perpendicular to the rolling plane and the others are inclined by 35.27° to the rolling plane. In the light of the mechanism of monocrystalline tension and the law of critical shear stress, $\sigma_s = \tau_k / \cos\Phi\cos\lambda$, where τ_k is the critical resolved shear stress, determined by the nature character of materials, and has nothing to do with the external force; the angle Φ is between normal direction of slip plane and central axis of external force; the angle λ is between slip direction and central axis of external force; $\cos\Phi\cos\lambda$ is Schmid factor. According to the relations of crystal directions in cubic crystal system, and the rules of operation of vector applied, the crystallographic directional indices of each tensile specimen orientations were figured out firstly, then the angle Φ and the angle λ of slip system {111}〈110〉 for various tensile specimen orientations were figured out, and the results of calculation are listed in Table 3 and Table 4. On the basis of this, Schmid factors of slip system {111}〈110〉 for various tensile orientations and the reciprocal of the maximum Schmid factor of every orientation were calculated and are listed in Table 5.

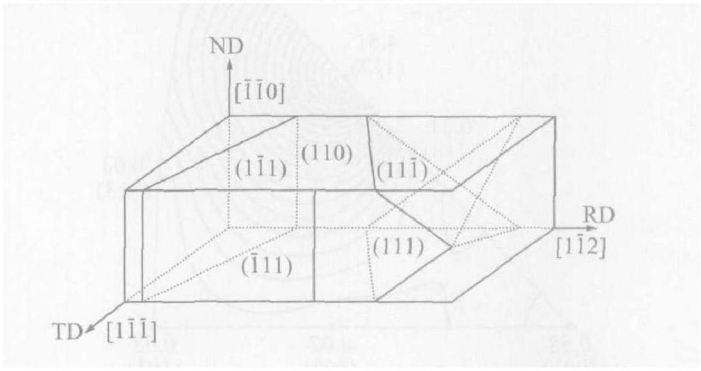

Fig. 6 Space relationship of four possible {111} slip planes with (110)[$1\bar{1}2$] texture

Table 3 Crystallographic directional indices of various tensile specimen orientations

Tensile specimen orientation	Crystallographic direction indice	
0°	[$1\bar{1}2$]	[$\bar{1}\bar{1}2$]
30°	[$1\bar{1}(8-3\sqrt{6})$]	[$\bar{1}1(3\sqrt{6}-8)$]
45°	[$1\bar{1}(3\sqrt{2}-4)$]	[$\bar{1}1(4-3\sqrt{2})$]
60°	[$1\bar{1}(3\sqrt{6}-8)/5$]	[$\bar{1}1(8-3\sqrt{6})/5$]
90°	[$1\bar{1}\bar{1}$]	[$\bar{1}11$]

As listed in Table 5, during the tensile testing, the specimens which orientate 0°, 30° and 90° with respect to the rolling direction, have bigger reciprocals of the maximum Schmid factors and higher yield strength than those of the specimens which orientate 45°, 60° with respect to the rolling direction. It is found that the results of this theoretical analysis agree well with the experimental results (Table 2). Therefore, the main cause which leads to the in-plane anisotropy of mechani-

Table 4 Angle Φ and angle λ of slip system {111}⟨110⟩ for various tensile specimen orientations

Slip system	Orientation of tensile specimen									
	0°		30°		45°		60°		90°	
	Φ/(°)	λ/(°)	Φ/(°)	λ/(°)	Φ/(°)	λ/(°)	Φ/(°)	λ/(°)	Φ/(°)	λ/(°)
$(1\bar{1}1)[110]$	19.47	90.00	10.53	90.00	25.53	90.00	40.53	90.00	70.53	90.00
$(1\bar{1}1)[011]$	19.47	73.22	10.53	80.89	25.53	68.09	40.53	55.75	70.53	35.26
$(1\bar{1}1)[\bar{1}01]$	19.47	73.22	10.53	80.89	25.53	68.09	40.53	55.75	70.53	35.26
$(\bar{1}11)[110]$	90.00	90.00	60.00	90.00	45.00	90.00	30.00	90.00	0	90.00
$(\bar{1}11)[0\bar{1}1]$	90.00	30.00	60.00	41.41	45.00	52.24	30.00	64.34	0	90.00
$(\bar{1}11)[101]$	90.00	30.00	60.00	41.41	45.00	52.24	30.00	64.34	0	90.00
$(111)[1\bar{1}0]$	61.87	54.74	76.02	24.74	84.40	9.74	86.96	5.26	70.53	35.26
$(111)[0\bar{1}1]$	61.87	30.00	76.02	41.41	84.40	52.24	86.96	64.34	70.53	90.00
$(111)[\bar{1}01]$	61.87	73.22	76.02	80.89	84.40	68.09	86.96	55.75	70.53	35.26
$(11\bar{1})[1\bar{1}0]$	61.87	54.74	76.02	24.74	84.40	9.74	86.96	5.26	70.53	35.26
$(11\bar{1})[011]$	61.87	73.22	76.02	80.89	84.40	68.09	86.96	55.75	70.53	35.26
$(11\bar{1})[101]$	61.87	30.00	76.02	41.41	84.40	52.24	86.96	64.34	70.53	90.00

Table 5 Schmid factors of slip system {111}⟨110⟩ for various tensile orientations and reciprocal of maximum Schmid factor of every orientation

Slip system	Orientation of tensile specimen				
	0°	30°	45°	60°	90°
$(1\bar{1}1)[110]$	0	0	0	0	0
$(1\bar{1}1)[011]$	0.272 2	0.155 6	0.336 8	0.427 7	0.272 2
$(1\bar{1}1)[\bar{1}01]$	0.272 2	0.155 6	0.336 8	0.427 7	0.272 2
$(\bar{1}11)[110]$	0	0	0	0	0
$(\bar{1}11)[0\bar{1}1]$	0	0.375 0	0.433 0	0.375 0	0
$(\bar{1}11)[101]$	0	0.375 0	0.433 0	0.375 0	0
$(111)[1\bar{1}0]$	0.272 2	0.219 4	0.096 2	0.052 8	0.272 2
$(111)[0\bar{1}1]$	0.408 2	0.181 2	0.059 8	0.022 9	0
$(111)[\bar{1}01]$	0.136 1	0.038 2	0.036 4	0.022 9	0.272 2
$(11\bar{1})[1\bar{1}0]$	0.272 2	0.219 4	0.096 2	0.052 8	0.272 2
$(11\bar{1})[011]$	0.136 1	0.038 2	0.036 4	0.029 8	0.272 2
$(11\bar{1})[101]$	0.408 2	0.181 2	0.059 8	0.022 9	0
Reciprocal of maximum Schmid factor	2.449 8	2.666 7	2.309 5	2.338 1	3.673 8

cal properties of 1545 alloy sheet is the crystallographic texture.

5 CONCLUSIONS

1) 1545 aluminum alloy sheet has remarkable in-plane anisotropy. The strength of specimens orientated 45° and 60° with respect to the rolling direction is lower than that of specimens orientated 0°, 30° and 90° with respect to the rolling direction. The elongation of specimens orientated 45° and 60° with respect to the rolling direction is higher than that of specimens orientated 0°, 30° and 90° with respect to the rolling direction. The transverse strength is higher than the longitudinal strength. At the same time, the in-plane anisotropy of the

elongation is higher than that of the yield strength and the tensile strength.

2) The main texture component in 1545 alloy sheet is {110}〈112〉 texture. It is the combined effects of the anisotropy of crystallography and microstructures that cause the in-plane anisotropy of mechanical properties, but the major cause is the crystallographic texture.

REFERENCES

[1] YIN Zhi-min, PAN Qing-lin, ZHANG Yong-hong. Effect of minor Sc and Zr on the microstructure and mechanical properties of Al-Mg based alloys[J]. Materials Science and Engineering, 2000, A280: 151-155.

[2] Vladivoj O, Margarita S. Resistance to recrystallization due to Sc and Zr addition to Al-Mg alloys[J]. Materials Characterization, 2001, 47: 157-162.

[3] Kendig K L, Miracle D B. Strengthening mechanism of Al-Mg-Sc-Zr alloy[J]. Acta Materialia, 2002, 50: 4165-4175.

[4] Lee S, Utsunomiya A, Akamatsu H, et al. Influence of scandium and zirconium on grain stability and superplastic ductilities in ultrafine-grained Al-Mg alloys[J]. Acta Materialia, 2002, 50: 553-564.

[5] Milman Y V, Lotsko D V, Sirko O L. 'Sc Effect' of improving mechanical properties in aluminium alloys [J]. Materials Science Forum, 2000, 331-337: 1107-1112.

[6] Reinhold B, Blanka L, Gerhard T. Effect of thermal exposure on the corrosion properties of an Al-Mg-Sc alloy sheet[J]. Materials Science Forum, 2000, 331-337: 1647-1652.

[7] Zaki A, Anwar U, Abdul-Aleem B J. The corrosion behavior of scandium Al 5052 in neutral sodium chloride solution[J]. Corrosion Science, 2001, 43: 1227-1243.

[8] Lathabai S, Lloyd P G. The effect of scandium on the microstructure, mechanical properties and weldability of a cast Al-Mg alloy[J]. Acta Materialia, 2002, 50: 4275-4292.

[9] Roder O, Wirtz T, Gysler A, et al. Fatigue properties of Al-Mg alloys with and without scandium[J]. Materials Science and Engineering, 1997, A234-236: 181-184.

[10] Jata K V, Hopkins A K, Rioja R J. Anisotropy and texture of Al-Li alloys[J]. Mat Sci Forum, 1996, 217-222: 647-652.

[11] Singh R K, Singh A K, Prasad N E. Texture and mechanical property anisotropy in an Al-Mg-Si-Cu alloy [J]. Materials Science and Engineering, 2000, A 277: 114-122.

[12] Takayuki S, Toshio K, Sin-ya K. Effects of texture and arrangements of dislocation cell walls on yield stress anisotropy in cold rolled and recovery annealed Al-Mg alloy sheets[J]. Mat Sci Forum, 2002, 396-402: 1055-1060.

[13] Vasudevan A K, Przystupa M A, Fricke Jr W G. Texture—microstructure effects in yield strength anisotropy of 2090 sheet alloy[J]. Scripta Metallurgica et Materialia, 1990, 24: 1429-1434.

[14] LI Shu-tang. Basis of Crystal X-ray Diffraction[M]. Beijing: Metallurgical Industry Press, 1990. 200. (in Chinese)

[15] TANG Ren-zheng. Basis of Physical Metallurgy[M]. Beijing: Metallurgical Industry Press, 1997. 228. (in Chinese)

(Edited by YANG Bing)